coatings

MDPI

Article

Chitosan Cross-Linked Bio-based Antimicrobial Polypropylene Meshes for Hernia Repair Loaded with Levofloxacin HCl via Cold Oxygen Plasma

Noor Sanbhal [1,2], Yan Li [1,*], Awais Khatri [2], Mazhar Peerzada [2] and Lu Wang [1,*]

[1] Key Laboratory of Textile Science and Technology of Ministry of Education, College of Textiles, Donghua University, 2999 North Renmin Road, Songjiang, Shanghai 201620, China; noor.sanbhal@faculty.muet.edu.pk

[2] Department of Textile Engineering, Mehran University of Engineering and Technology, Jamshoro 76062, Sindh, Pakistan; awais.khatri@faculty.muet.edu.pk (A.K.); mazhar.peerzada@faculty.muet.edu.pk (M.P.)

* Corresponding: yanli@dhu.edu.cn (Y.L.); wanglu@dhu.edu.cn (L.W.); Tel./Fax: +86-21-6779-2637 (L.W.)

Received: 18 December 2018; Accepted: 26 February 2019; Published: 4 March 2019

Abstract: Polypropylene (PP) large pore size nets have been most widely used implants for hernia repair. Nevertheless, the growth of bacteria within PP mesh pores after operation is a major reason of hernia recurrence. Secondly, pre-operative prophylaxis during mesh implantation has failed due to the hydrophobic nature of PP meshes. Herein, chitosan cross-linked and levofloxacin HCl incorporated, antimicrobial PP mesh devices were prepared using citric acid as a bio-based and green cross-linking agent. The inert PP mesh fibers were surface activated using O_2 plasma treatment at low pressure. Then, chitosan of different molecular weights (low and medium weight) were cross-linked with O_2 plasma activated surfaces using citric acid. Scanning electron microscopy (SEM), energy dispersive X-ray (EDX) spectroscopy, and Fourier transform infrared (FTIR) spectroscopy confirmed that chitosan was cross-linked with O_2 plasma-treated PP mesh surfaces and formed a thin layer of chitosan and levofloxacin HCl on the PP mesh surfaces. Moreover, antimicrobial properties of chitosan and levofloxacin HCl-coated PP meshes were investigated using an agar plate release method. The coated PP meshes demonstrated excellent antimicrobial inhibition zone up to 10 mm. Thus, modified PP meshes demonstrated sustained antimicrobial properties for six continuous days against *Staphylococcus aureus* (*SA*) and *Escherichia coli* (*EC*) bacteria.

Keywords: antimicrobial; polypropylene; chitosan; citric acid; cross-linked; cold plasma

1. Introduction

Light weight polypropylene (PP) mesh implantation for hernia repair has been performed to reinforce damaged tissues of the abdominal wall [1]. The recurrence rate of repaired hernia has been reduced marginally by using synthetic PP implants [2–4]. However, after PP mesh implantation, infection can be rare (1%–4%) [5,6], but subsequent failure of hernia mesh devices cannot be undervalued [7,8]. Reasons for infection may be the colonization of bacteria of the uneven knitting surfaces of PP meshes which may cause fistula formation around its pore size and result in the formation of granuloma [9]. In fact, pre-operative prophylaxis has no impact on mesh infection prevention because of non-absorbent PP characteristics [10,11]. Mesh infection is difficult to cure, considering continuous antibiotic therapy for a longer duration time, or it may result in the removal of implants [12]. Therefore, mesh infections should be cured in the very early stages, during mesh implantation [13].

Plasma treatment is an effective method used to modify the surfaces of biomaterials [14–16]. Among other plasma processes, cold oxygen plasma has been reported as a suitable process [17–19]

to modify PP fiber surfaces without changing bulk properties [20,21]. However, different surface coatings for PP meshes have been reported [15,22–26], but few authors have suggested green bio-based drug carriers such as chitosan for prolonged antimicrobial effects [27–29]. Chitosan is obtained from chitin, a very cheap product commonly available as shellfish waste. Chitosan is a natural polymer which has great importance as a biomaterials polymer due to its exceptional biological properties, such as being a non-toxic biodegradable and biocompatible drug carrier. Chitosan is commonly used in biomedical devices because of its excellent antimicrobial properties against gram-positive and gram-negative bacteria. Moreover, it is a carbohydrate used as an advanced active species to coordinate with transit metals [29]. Chitosan can carry broad spectrum soluble antibiotic drugs and release them after a suitable duration of time for mesh infection prevention. Thus, the polymer having antibiotic properties itself and being used as an antibiotic drug carrier may be of great interest in the application of hernia mesh surface functional materials [27]. The existence of hydroxyl and amino groups on chitosan gives it the advantage of being able to cross-link with a number of chemicals to form amide and ester bonds [30–32]. Moreover, levofloxacin HCl is a soluble drug commonly used for infection prevention with suitable release properties and it is capable of inhibiting both types (gram-negative and gram-positive) of bacteria [33].

Cakmak et al. have reported satisfactory results of chitosan- and triclosan-coated PP meshes [34]. Nevertheless, growing concern around triclosan limits its application [35]. Moreover, Avetta et al. have reported surface functionalisation of PP meshes with chitosan and ciprofloxacin but with antibacterial properties lasting only four days [27].

However, chitosan can be cross-linked using different cross-linking agents such as formaldehyde and glutaraldehyde. Nevertheless, these chemicals are toxic and the biocompatibility of the yield product is the primary and most basic requirement for all medical devices. Citric acid has been used for biomedical applications [36–38] and it has been reported that citric acid is a safe and bio-based green crosslinking agent for chitosan polymers [39].

In our previous work, we treated PP meshes with cold oxygen plasma, after which two steps grafting (with hexamethylene diisocyanate and cyclodextrin) were performed for β-cyclodextrin incorporation; afterwards, levofloxacin HCl was loaded into the β-cyclodextrins (CD) cavity [40]. Herein, a simple textile based one bath padding method was selected to incorporate a chitosan and levofloxacin HCl coating onto oxygen plasma-treated meshes using citric acid.

Polypropylene (PP) meshes were first surface activated using O_2 plasma treatment at low pressure, after which the PP meshes were padded (pick up 90%) with a prepared solution of chitosan and levofloxacin HCl containing citric acid as a cross-linking agent, as shown in Figure 1. The padded PP mesh devices were dried (40 °C) and cured (70 °C) in an oven for 10 min. The surface morphology, chemical composition, and structural changes of the plasma treated chitosan and levofloxacin HCl-coated PP meshes were characterized using scanning electron microscopy (SEM), energy dispersive X-ray (EDX) spectroscopy, and Fourier transform infrared (FTIR) spectroscopy. Results revealed that the PP mesh was connected with chitosan through the oxygen plasma treatment. Thus, a thin layer of chitosan and levofloxacin HCl was observed on the surfaces of the PP meshes. Furthermore, antimicrobial properties of chitosan and levofloxacin HCl-coated PP meshes were performed via an agar diffusion plate by release properties. Thus, the chitosan and levofloxacin-modified devices demonstrated an excellent antimicrobial zone of inhibition and sustained antimicrobial release properties for six continuous days.

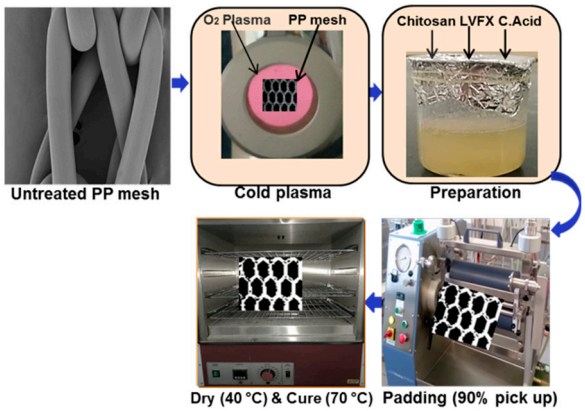

Figure 1. Illustrations and experimental design of chitosan and levofloxacin HCl-coated polypropylene (PP) meshes.

2. Materials and Methods

2.1. Materials

Light weight (27 g/m^2) PP mono filament meshes with pore sizes 2.5 mm × 3.5 mm were purchased from Nantong Newtec Textile and Chemical Fiber Co. Ltd. China (Nantong, China). Levofloxacin hydrochloride (98%) was purchased from Energy Chemicals Shanghai China (Shanghai, China). Citric acid monohydrate and acetic acid were received of analytical reagents.

2.2. Surface Functionalization of PP with Oxygen Plasma

PP mesh devices (10 cm × 10 cm) were functionalized using cold oxygen plasma (HD-300) at low pressure. All samples were surface activated for 5 min at 45 W. The oxygen gas flow was kept at less than 0.2 bar.

2.3. Preparation of Chitosan and Levofloxacin HCl Solution and Coating onto PP Meshes

The antibacterial solution was prepared following the pad dry method described by Avetta et al. [27]. Chitosan of low molecular weight (CH-LMW) and medium molecular weight (CH-MMW) were dissolved in deionized water with acetic acid. The solution was stirred for 12 h at room temperature using a magnetic stirrer at 150 rpm. Then, levofloxacin HCl was poured into the solution of chitosan and stirred for a further 2 h to mix the antimicrobial homogeneously. The overall concentration maintained in the solution was chitosan 2.0 wt % (low and medium), levofloxacin HCl (0.2%), citric acid (2%) and acetic acid (0.5%) was added to dissolve the chitosan.

Plasma-treated meshes were dipped in the chitosan solution and padded through horizontal padding at 90% pick up (1.2 bar pressure). The mesh devices were padded twice to get an even coating on the whole mesh surfaces. Moreover, coated samples were first dried at 40 °C and then cured at 70 °C for 10 min to perform the cross-linking of chitosan with the plasma-treated fibers.

3. Characterization

3.1. SEM and EDX

Chitosan and levofloxacin HCl-modified PP meshes were evaluated for surface morphology by scanning electron microscopy (Quanta SEM 250, FEI, Waltham, MA, USA). Samples were used for coating platinum (Pt) before SEM scanning. Moreover, element analysis of chitosan and levofloxacin HCl-modified PP mesh devices was performed using energy dispersive X-ray spectroscopy (ISIS 300, Oxford Instruments, Oxfordshire, UK).

3.2. FTIR

The surface structures of the modified and control meshes were investigated using Fourier transform infrared spectroscopy (Nicolet 6700, Thermo Fisher Scientific, Waltham, MA, USA) of attenuated total reflection (ATR). The FTIR range used to analysis the structure was between 4000–500 cm^{-1}.

3.3. Differential Scanning Calorimetry (DSC) and X-ray Diffraction (XRD)

A DSC (Pyris, Perkin Elemer, Waltham, MA, USA) test was performed to get the melting temperature of the chitosan and levofloxacin HCl-coated and untreated samples. All samples were scanned in the temperature range of 30–300 °C at 20 °C/min.

Moreover, chitosan and levofloxacin-coated and untreated samples were characterized using an X-ray diffractometer (Rigaku D/MAX 2550/PC, Tokyo, Japan). The range of crystallization analysis was 5° to 60° (2θ) and the testing rate was set at 0.02°/min.

3.4. Antibacterial Activity

The antibacterial activity of chitosan (low and medium molecular weight) was investigated using a simple agar diffusion plate test method. A specific amount of 400 µL of bacteria (*Staphylococcus aureus* (*SA*) and *Escherichia coli* (*EC*)) of 1×10^8 colony forming units (CFU)/mL was poured on agar plates. Then, treated and untreated samples (1 cm × 1 cm) were placed onto the center of the agar plates and all samples were incubated in an oven at 37 °C for 24 h [41]. The zone of inhibition of each sample was measured in all four directions and described as an average antibacterial inhibition zone value. The formula for the zone of inhibition was $C = (K - B)/2$ where C = inhibition zone, K = inhibition zone after incubation (24 h), and B is the original sample (1 × 1) without antibacterial activity.

Furthermore, PP-untreated and chitosan-treated samples were analyzed for their antibacterial release properties. Each day samples were transferred to new agar plates and fresh bacteria were poured. Thus, after 24 h the inhibition zone was measured and compared with the previous one. The antibacterial release performance was continued until the modified meshes sustained antibacterial activity.

3.5. Statistical Analysis

The standard deviation and mean are reported in Figure 8. However, standard bars in the figures represent standard deviation. One-way single factor ANOVA was performed to find out the actual differences for each sample. The figure data is marked with $p < 0.001$ (***), $p < 0.01$ (**), and $p < 0.05$ (*). Thus, the value of $p < 0.05$ (*) was chosen as a confidence interval value.

4. Results and Discussion

4.1. Chitosan and Levofloxacin Coating onto PP Mesh Surfaces

Chitosan was cross-linked with PP meshes using citric acid monohydrate, as shown in the reaction scheme (Figure 2). Chitosan of low molecular weight and chitosan of medium molecular weight with levofloxacin HCl were prepared using acetic acid and stirred for 12 h, after which citric acid monohydrate was poured into the solutions prior to 2 h of coating. The coating solutions containing CH-LMW and CH-MMW were separately padded onto O_2 plasma activated surfaces of PP meshes. The coated meshes were dried and cured at 70 °C for 10 min to cross-link chitosan with the PP mesh surfaces. The average corresponding weight of the samples of low molecular weight (2.05 ± 1.3%) and medium molecular weight (4.1% ± 0.8%) was increased. The result was that a thin layer of chitosan with levofloxacin HCl was obtained onto the plasma activated PP fiber surfaces. Thus, plasma-treated PP meshes of CH-MMW received more amounts of surface coating in comparison to CH-MMW.

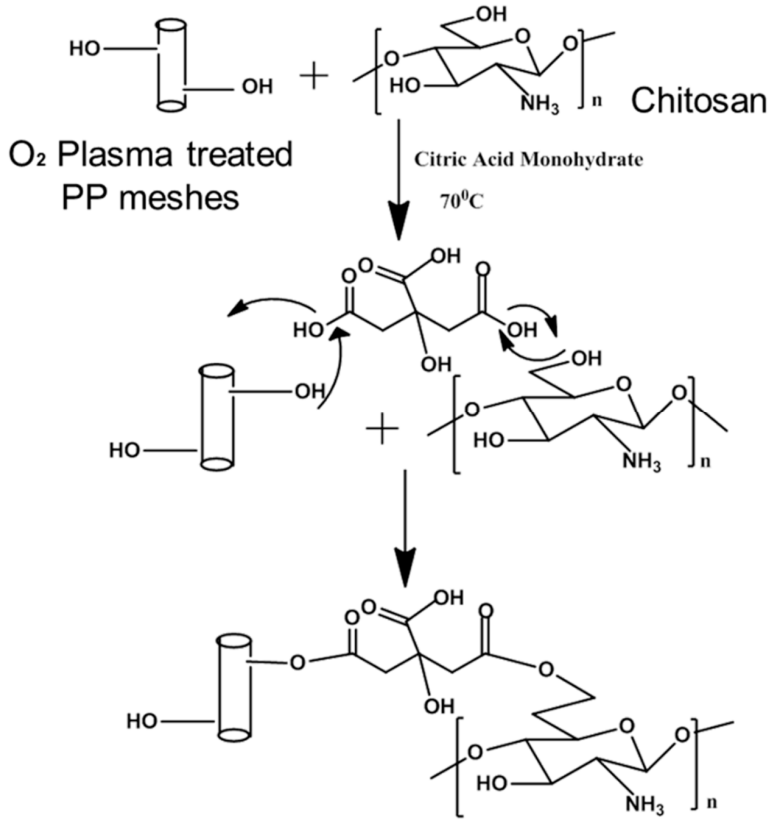

Figure 2. Reaction scheme of cross-linked chitosan with oxygen plasma-treated PP meshes using citric acid.

4.2. Surface Morphology of Chitosan and Levofloxacin HCl-Modified PP Meshes

SEM images of chitosan and levofloxacin HCl-modified plasma-treated and -untreated PP meshes are shown in Figure 3. It can be observed that the untreated PP meshes display noticeable line marks on their surfaces (Figure 3a) with bright surface structures, but after oxygen plasma treatment such line marks are missing, showing (Figure 3b) relatively dull and even surfaces. The plasma-treated fibers have regular surfaces in comparison to the untreated meshes. Moreover, the low molecular weight chitosan and levofloxacin-coated meshes display (Figure 3c) an even thin layer across the whole spherical diameter of the fibers. However, it can be observed that the medium weight chitosan and levofloxacin HCl completely coated the (Figure 3d) plasma-activated PP fibers with a thick and sticky layer. It can be seen that the sticky layer (the CH-MMW) stretches across the whole surface of the PP fibers, showing a more even coating than the CH-LMW coating. Thus, it can be summarized that medium molecular weight chitosan can coat PP fibers more effectively. The reason for the thick and even surface coating may be the oxygen plasma treatment, which may enhance the adhesion of the chitosan and levofloxacin HCl coating [19].

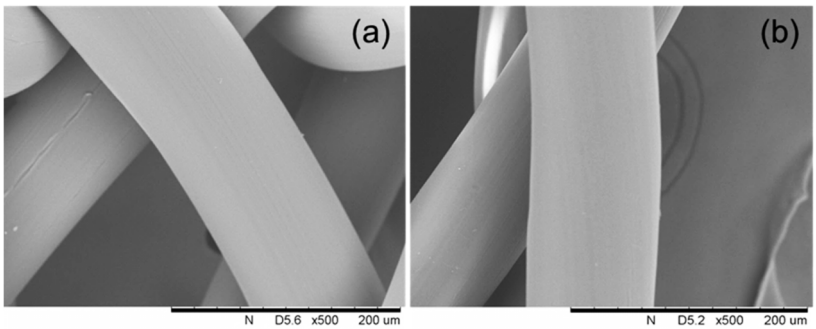

Figure 3. *Cont.*

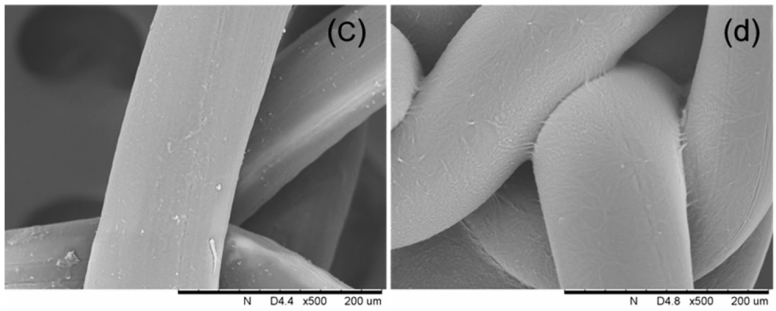

Figure 3. Scanning electron microscopy (SEM) images: (**a**) PP-untreated, (**b**) oxygen plasma-treated, (**c**) chitosan of low molecular weight (CH-LMW)-coated PP meshes, and (**d**) chitosan of medium molecular weight (CH-MMW) and levofloxacin HCl-coated PP meshes. All samples were scanned at a magnification of 500×.

4.3. Characterization of Chitosan and Levofloxacin HCl-Modified PP Devices

Figure 4 displays energy dispersive X-ray spectroscopy peaks for the identification of the surface chemical structures of the PP meshes and the plasma-treated and chitosan and levofloxacin HCl-modified mesh devices. The PP control meshes displayed a 100% carbon peak at 0.4 keV. Nevertheless, the plasma-treated meshes confirmed a carbon atom at a similar 0.4 keV mark but an additional oxygen (O) atom peak (2.9%) was observed at 0.7 keV. Moreover, CH-LMW-coated PP meshes displayed an increase in oxygen (13.31%) atoms and additionally, two peaks of nitrogen and fluorine can be observed around 0.8 keV. Furthermore, medium molecular weight chitosan and levofloxacin HCl-coated samples displayed same atoms similar to CH-LMW but with increased atomic weight percentages, indicating the good efficiency of the chitosan layer when making it onto the PP surfaces. These results are in accord with published paper [27], except that we received an additional peak of levofloxacin HCl, which is the most commonly used antimicrobial for infection prevention. Thus, cold oxygen plasma is shown to be an important process regarding enhancing surface adhesion for the coating of chitosan and levofloxacin HCl onto PP mesh surfaces.

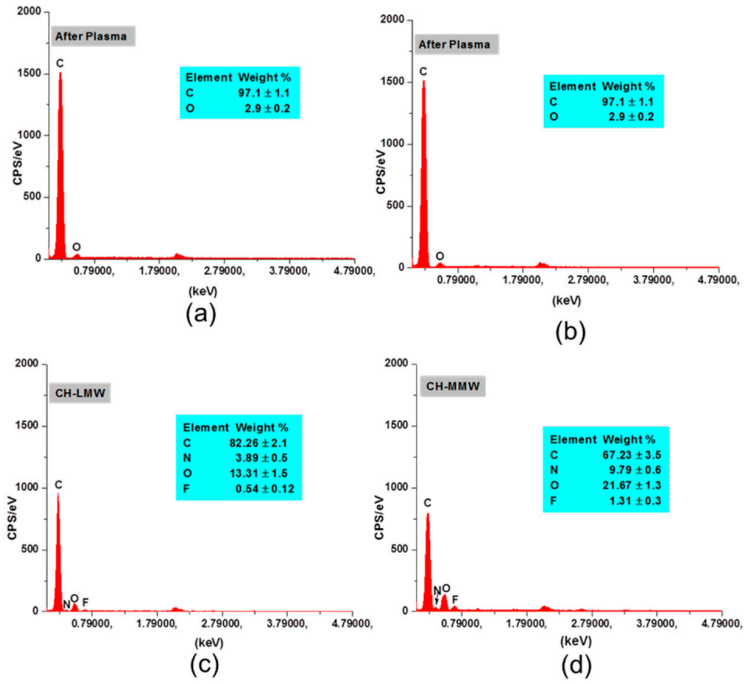

Figure 4. Energy dispersive X-ray (EDX) spectra: (**a**) PP control, (**b**) oxygen plasma-functionalized, (**c**) low molecular weight chitosan and levofloxacin, and (**d**) medium molecular weight chitosan and levofloxacin HCl-coated PP meshes.

FTIR spectra of chitosan and levofloxacin HCl-coated meshes are shown in Figure 5. The PP control fibers displayed identical peaks at 2951, 2918, 1453, and 1378 cm^{-1} [42,43]. However, when excluding the PP fiber original peaks, a new peak (Figure 5a) at 3347 cm^{-1} may be observed, which may be due to the oxygen plasma treatment which provides an OH group to the PP fiber surfaces. Moreover, as shown in Figure 5b, chitosan-coated modified meshes show a slight change in the vibration band at 3398 cm^{-1}, but the peak height was more in alignment with the oxygen plasma-treated fibers. The chitosan-coated modified PP meshes also show an additional cross-linking peak at 1715 cm^{-1}, which may be due to the formation of a carbonyl group. However, amide I and amide II were observed at 1625 and 1215 cm^{-1}, respectively. The C–O stretch of chitosan was seen within the fingerprint region at 1070 cm^{-1} for the medium-weight chitosan-coated meshes. These results are in accord with published paper [27], but most notably in our work we found extra peaks at 1715 cm^{-1}, which are due to the formation of a carbonyl group. The reason for the formation of a peak at 1070 cm^{-1} specially for the CH-MMW meshes may be due to the better coating efficiency of chitosan onto the oxygen-treated PP meshes in comparison with the CH-LMW coating.

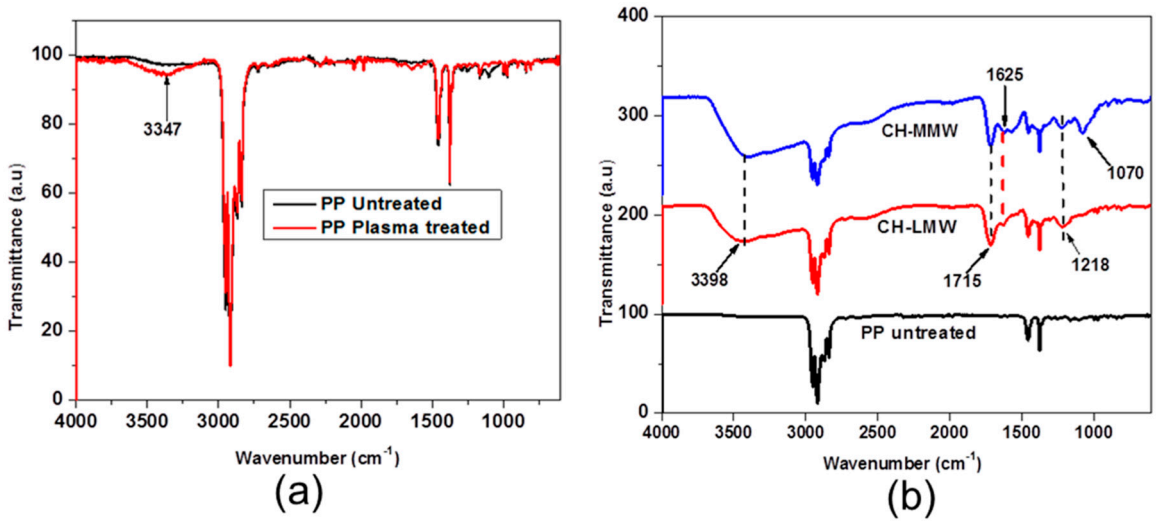

Figure 5. Fourier transform infrared (FTIR) spectra (attenuated total reflection (ATR)): (**a**) PP control and oxygen plasma-treated PP meshes; (**b**) PP control, CH-LMW, and CH-MMW and levofloxacin-coated PP meshes.

4.4. Thermal and Structural Properties

As shown in Figure 6a, the PP meshes without treatment, and those coated with chitosan and levofloxacin HCl, have no identical differences except that the control PP mesh has more peak height. Moreover, all three samples—PP control, CH-LMW, and CH-MMW—have almost the same melting temperatures, these being 148.5, 148.9, and 149.05 °C, respectively. Thus, there is a slight increase in melting temperature as chitosan coating is applied to the PP mesh surfaces. Overall, there is no difference in melting temperature between the treated and untreated PP meshes.

Figure 6b displays XRD patterns of chitosan-coated and non-coated PP meshes. It can be observed that the PP meshes coated with low molecular weight chitosan, medium molecular weight chitosan, and those which are untreated exhibited similar pattern peaks and crystal structures for the 2θ range 5°–60°. Therefore, there are no identical structural changes before and after the surface modification of the PP meshes.

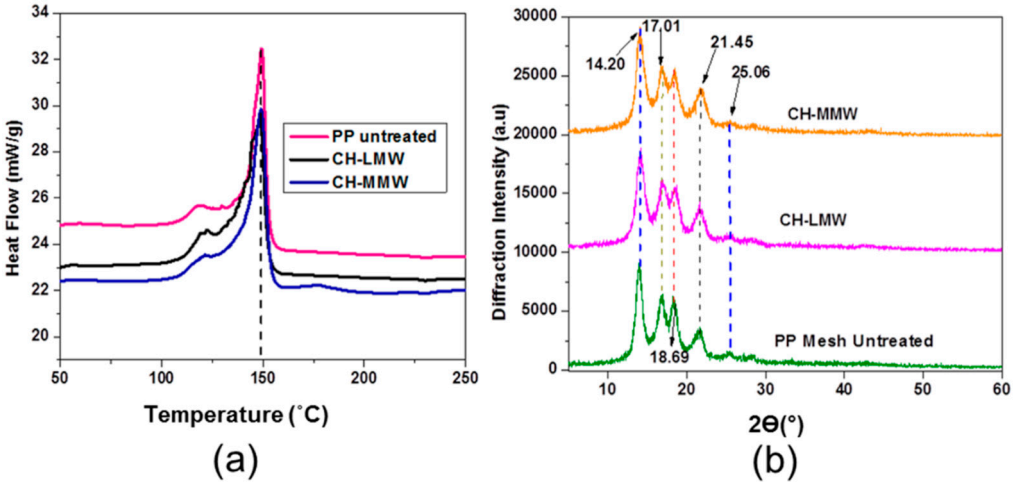

Figure 6. Thermal and structural properties: (**a**) differential scanning calorimetry (DSC) analysis and (**b**) X-ray diffraction (XRD) patterns of treated and untreated PP meshes.

4.5. Antibacterial Activity

Antibacterial properties of the chitosan and levofloxacin HCl (CH-LMW and CH-MMW) and untreated meshes are shown in Figure 7. Untreated PP mesh fibers were unable to resist bacterial (*EC* and *SA*) growth. Thus, there is no inhibition zone (Figure 7a,b) around the PP control samples. Nevertheless, the CH-LMW and levofloxacin HCl-coated PP meshes demonstrated suitable antibacterial properties. The CH-LMW-coated meshes displayed an average inhibition zone of 8.1 and 8.6 mm for *SA* and *EC*, respectively. However, in the case of the CH-MMW and levofloxacin coated samples, these demonstrated better average inhibition zones of 10.1 and 10.9 mm for *SA* and *EC*, respectively. Thus, the CH-MMW samples demonstrated a bigger average inhibition zone than the CH-LMW samples.

Thus, it was confirmed that PP control does not exhibit antibacterial properties. For this reason, the CH-LMW and CH-MMW samples were assessed for their antimicrobial release properties. Both samples (CH-LMW and CH-MMW) were further tested (Figure 8) against *SA* and *EC* by a release method. As shown in Figure 8a, the average initial inhibition zones for the CH-LMW samples for the first day against *SA* and *EC* were 8.01 and 8.533 mm, respectively. CH-LMW demonstrated antibacterial release properties for four days against *SA* and *EC* bacteria. *EC* displayed a bigger inhibition zone than *SA* over the four days. However, the minimum inhibition zones for *SA* (0.5 mm) and *EC* (0.8 mm) were measured on the fourth day.

Moreover, antimicrobial properties of CH-MMW samples sustained (Figure 8b) for 6 days. CH-MMW samples displayed 11 and 10.1 mm inhibition zone for *SA* and *EC*, respectively. This was greater inhibition zone than CH-LMW. However, similarly like CH-LMW, EC shown bigger inhibition zone during entire 6 days but on 4th day zone of inhibition was almost same for *SA* and *EC*. Minimum average inhibition zone for SA (0.3 mm) and EC (1.2 mm) were seen on day 6. According to previous published papers author reported chitosan functionalized PP meshes [29] only 4 days of drug release was achieved [27]. However, antimicrobial results for CH-MMW shown better results and sustained antibacterial release up to 6 days. This may be due to the surface functionalization of PP meshes with oxygen plasma as literature described that cold oxygen plasma is a more suitable surface treatment than other plasma treatments [19,40]. Secondly citric acid is a good cross-linker and has been used commonly to connect hydroxyl group with chitosan [30]. Therefore, formation of hydroxyl group on PP surfaces given advantage to connect oxygen plasma treated PP fibers with chitosan. The results of SEM, FTIR and antimicrobial release method proved that chitosan and levofloxacin layer was cross-linked with plasma activated surfaces which gave better results of antimicrobial.

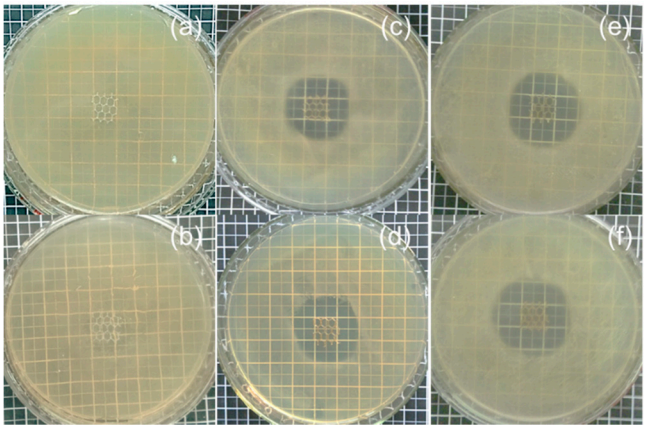

Figure 7. Antibacterial activity by inhibition zone: (**a**,**b**) PP control, (**c**,**d**) low molecular weight chitosan and levofloxacin-coated, (**e**,**f**) medium molecular weight chitosan and levofloxacin HCl-coated. Note: the top row is *SA* and the bottom row is *EC*.

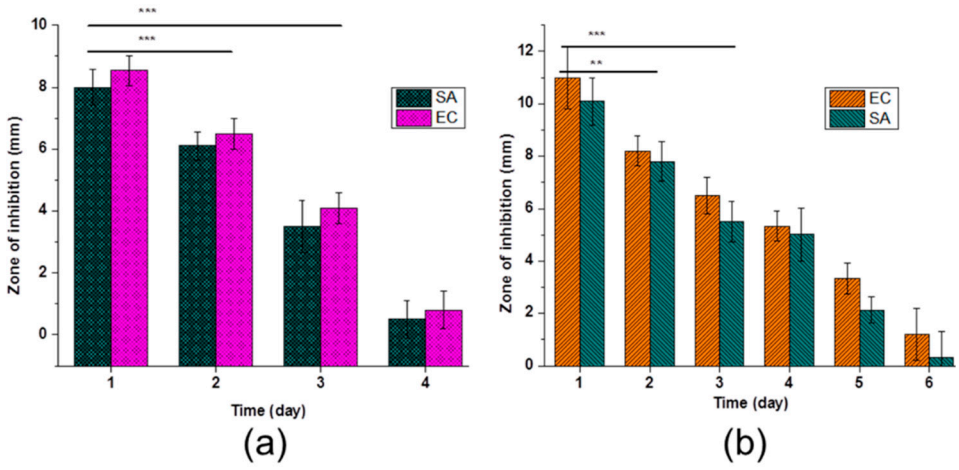

Figure 8. Antibacterial activity by release method (**a**) low molecular weight chitosan and levofloxacin coated CH-LMW (**b**) Medium molecular weight and levofloxacin HCL coated PP meshes (CH-MMW).

5. Conclusions

In this study, chitosan of low molecular weight and chitosan of medium molecular weight with levofloxacin HCl were successfully coated onto oxygen plasma-treated PP mesh fiber surfaces. Plasma activation created adhesion on the surfaces of the PP fibers, which was utilized to connect PP meshes with chitosan in presence of citric acid. The result was a thin layer of chitosan and levofloxacin HCl coating the PP meshes. FTIR confirmed that chitosan was successfully attached and cross-linked with the PP mesh fibers.

Moreover, the chitosan and levofloxacin HCl-modified PP meshes demonstrated excellent antimicrobial inhibition zones and antimicrobial release properties which were sustained for six days. Thus, a green and bio-based chitosan with suitable antimicrobial properties could be used for mesh infection prevention during hernia repair.

Author Contributions: Conceptualization, N.S. and Y.L.; Methodology, N.S.; Software, N.S.; Validation, A.K. and N.S.; Writing—Original Draft Preparation, M.P. and N.S.; Writing-Review and Editing, L.W.

Funding: This work was supported by the 111 project "Biomedical Textile Material (No. B07024) Science and Technology", the National Key Research Development Program (No. 2016YFB 0303300-03) of China, and the Fundamental Research (Nos. 17D110111 and 2232018G-01) Funds for the Central Universities.

Acknowledgments: Thanks to Rafique Ahmed lakho for his help during the experiments.

Conflicts of Interest: The authors declare no conflict of interest.

References

1. Miao, L.; Wang, F.; Wang, L.; Zou, T.; Brochu, G.; Guidoin, R. Physical characteristics of medical textile prostheses designed for hernia repair: A comprehensive analysis of select commercial devices. *Materials* **2015**, *8*, 8148–8168. [CrossRef] [PubMed]
2. Greca, F.; Paula, J.; Biondo-Simões, M.; Costa, F.; Silva, A.; Time, S.; Mansur, A. The influence of differing pore sizes on the biocompatibility of two polypropylene meshes in the repair of abdominal defects. *Hernia* **2001**, *5*, 59–64. [PubMed]
3. Hazebroek, E.J.; Ng, A.; Yong, D.H.; Berry, H.; Leibman, S.; Smith, G.S. Evaluation of lightweight titanium-coated polypropylene mesh (TiMesh) for laparoscopic repair of large hiatal hernias. *Surg. Endosc.* **2008**, *22*, 2428–2432. [CrossRef] [PubMed]
4. Jerabek, J.; Novotny, T.; Vesely, K.; Cagas, J.; Jedlicka, V.; Vlcek, P.; Capov, I. Evaluation of three purely polypropylene meshes of different pore sizes in an onlay position in a New Zealand white rabbit model. *Hernia* **2014**, *18*, 855–864. [CrossRef] [PubMed]
5. Perez-Kohler, B.; Bayon, Y.; Bellon, J.M. Mesh infection and hernia repair: A review. *Surg. Infect.* **2016**, *17*, 124–137. [CrossRef] [PubMed]
6. Guillaume, O.; Perez-Tanoira, R.; Fortelny, R.; Redl, H.; Moriarty, T.F.; Richards, R.G.; Eglin, D.; Petter Puchner, A. Infections associated with mesh repairs of abdominal wall hernias: Are antimicrobial biomaterials the longed-for solution? *Biomaterials* **2018**, *167*, 15–31. [CrossRef] [PubMed]
7. Kulaga, E.; Ploux, L.; Balan, L.; Schrodj, G.; Roucoules, V. Mechanically responsive antibacterial plasma polymer coatings for textile biomaterials. *Plasma Process. Polym.* **2014**, *11*, 63–79. [CrossRef]
8. Knetsch, M.L.; Koole, L.H. New strategies in the development of antimicrobial coatings: The example of increasing usage of silver and silver nanoparticles. *Polymers* **2011**, *3*, 340–366. [CrossRef]
9. Sanbhal, N.; Miao, L.; Xu, R.; Khatri, A.; Wang, L. Physical structure and mechanical properties of knitted hernia mesh materials: A review. *J. Ind. Text.* **2018**, *48*, 333–360. [CrossRef]
10. Mazaki, T.; Mado, K.; Masuda, H.; Shiono, M.; Tochikura, N.; Kaburagi, M. A randomized trial of antibiotic prophylaxis for the prevention of surgical site infection after open mesh-plug hernia repair. *Am. J. Surg.* **2014**, *207*, 476–484. [CrossRef] [PubMed]
11. Mazaki, T.; Mado, K.; Masuda, H.; Shiono, M. Antibiotic prophylaxis for the prevention of surgical site infection after tension-free hernia repair: A Bayesian and frequentist meta-analysis. *J. Am. Coll. Surg.* **2013**, *217*, 788–801. [CrossRef] [PubMed]
12. Zhang, Z.; Tang, J.; Wang, H.; Xia, Q.; Xu, S.; Han, C.C. Controlled antibiotics release system through simple blended electrospun fibers for sustained antibacterial effects. *ACS Appl. Mater. Interfaces* **2015**, *7*, 26400–26404. [CrossRef] [PubMed]
13. Guillaume, O.; Garric, X.; Lavigne, J.P.; Van Den Berghe, H.; Coudane, J. Multilayer, degradable coating as a carrier for the sustained release of antibiotics: Preparation and antimicrobial efficacy in vitro. *J. Control. Release* **2012**, *162*, 492–501. [CrossRef] [PubMed]
14. Khelifa, F.; Ershov, S.; Habibi, Y.; Snyders, R.; Dubois, P. Free-radical-induced grafting from plasma polymer surfaces. *Chem. Rev.* **2016**, *116*, 3975–4005. [CrossRef] [PubMed]
15. Nisticò, R.; Rosellini, A.; Rivolo, P.; Faga, M.G.; Lamberti, R.; Martorana, S.; Castellino, M.; Virga, A.; Mandracci, P.; Malandrino, M.; et al. Surface functionalisation of polypropylene hernia-repair meshes by RF-activated plasma polymerisation of acrylic acid and silver nanoparticles. *Appl. Surf. Sci.* **2015**, *328*, 287–295. [CrossRef]
16. Nisticò, R.; Magnacca, G.; Faga, M.G.; Gautier, G.; D'Angelo, D.; Ciancio, E.; Lamberti, R.; Martorana, S. Effect of atmospheric oxidative plasma treatments on polypropylenic fibers surface: Characterization and reaction mechanisms. *Appl. Surf. Sci.* **2013**, *279*, 285–292. [CrossRef]
17. Jelil, R.A. A review of low-temperature plasma treatment of textile materials. *J. Mater. Sci.* **2015**, *50*, 5913–5943. [CrossRef]
18. Lai, J.; Sunderland, B.; Xue, J.; Yan, S.; Zhao, W.; Folkard, M.; Michael, B.D.; Wang, Y. Study on hydrophilicity of polymer surfaces improved by plasma treatment. *Appl. Surf. Sci.* **2006**, *252*, 3375–3379. [CrossRef]
19. Sorrentino, L.; Carrino, L.; Napolitano, G. Oxygen cold plasma treatment on polypropylene: Influence of process parameters on surface wettability. *Surf. Eng.* **2013**, *23*, 247–252. [CrossRef]
20. Shishoo, R. *Plasma Technologies for Textiles*; Woodhead publishing limited: Sawston, UK, 2007.

21. Fauland, G.; Constantin, F.; Gaffar, H.; Bechtold, T. Production scale plasma modification of polypropylene baselayer for improved water management properties. *J. Appl. Polym. Sci.* **2015**, *132*, 41294. [CrossRef]
22. Perez-Kohler, B.; Fernandez-Gutierrez, M.; Pascual, G.; Garcia-Moreno, F.; San Roman, J.; Bellon, J.M. In vitro assessment of an antibacterial quaternary ammonium-based polymer loaded with chlorhexidine for the coating of polypropylene prosthetic meshes. *Hernia* **2016**, *20*, 869–878. [CrossRef] [PubMed]
23. Labay, C.; Canal, J.M.; Modic, M.; Cvelbar, U.; Quiles, M.; Armengol, M.; Arbos, M.A. Antibiotic-loaded polypropylene surgical meshes with suitable biological behaviour by plasma functionalization and polymerization. *Biomaterials* **2015**, *71*, 132–144. [CrossRef] [PubMed]
24. Harth, K.C.; Rosen, M.J.; Thatiparti, T.R.; Jacobs, M.R.; Halaweish, I.; Bajaksouzian, S.; Furlan, J.; von Recum, H.A. Antibiotic-releasing mesh coating to reduce prosthetic sepsis: An in vivo study. *J. Surg. Res.* **2010**, *163*, 337–343. [CrossRef] [PubMed]
25. Gorgieva, S.; Modic, M.; Dovgan, B.; Kaisersberger-Vincek, M.; Kokol, V. Plasma-activated polypropylene mesh-gelatin scaffold composite as potential implant for bioactive hernia treatment. *Plasma Process. Polym.* **2015**, *12*, 237–251. [CrossRef]
26. Muzio, G.; Miola, M.; Perero, S.; Oraldi, M.; Maggiora, M.; Ferraris, S.; Vernè, E.; Festa, V.; Festa, F.; Canuto, R.A.; et al. Polypropylene prostheses coated with silver nanoclusters/silica coating obtained by sputtering: Biocompatibility and antibacterial properties. *Surf. Coat. Technol.* **2017**, *319*, 326–334. [CrossRef]
27. Avetta, P.; Nisticò, R.; Faga, M.G.; D'Angelo, D.; Boot, E.A.; Lamberti, R.; Martorana, S.; Calza, P.; Fabbri, D.; Magnacca, G. Hernia-repair prosthetic devices functionalised with chitosan and ciprofloxacin coating: Controlled release and antibacterial activity. *J. Mater. Chem. B* **2014**, *2*, 5287–5294. [CrossRef]
28. Udpa, N.; Iyer, S.R.; Rajoria, R.; Breyer, K.E.; Valentine, H.; Singh, B.; McDonough, S.P.; Brown, B.N.; Bonassar, L.J.; Gao, Y. Effects of chitosan coatings on polypropylene mesh for implantation in a rat abdominal wall model. *Tissue Eng. Part A* **2013**, *19*, 2713–2723. [CrossRef] [PubMed]
29. Nisticò, R.; Faga, M.G.; Gautier, G.; Magnacca, G.; D'Angelo, D.; Ciancio, E.; Piacenza, G.; Lamberti, R.; Martorana, S. Physico-chemical characterization of functionalized polypropylenic fibers for prosthetic applications. *Appl. Surf. Sci.* **2012**, *258*, 7889–7896. [CrossRef]
30. Aubert-Viard, F.; Martin, A.; Chai, F.; Neut, C.; Tabary, N.; Martel, B.; Blanchemain, N. Chitosan finishing nonwoven textiles loaded with silver and iodide for antibacterial wound dressing applications. *Biomed. Mater.* **2015**, *10*, 015023. [CrossRef] [PubMed]
31. Shweta, A.; Sonia, P. Pharmaceutical relevance of cross-linked chitosan in microparticulate drug delivery. *Int. Res. J. Pharm.* **2013**, *4*, 45–51.
32. Abraham, S.; Rajamanickam, D.; Srinivasan, B. Preparation, characterization and cross-linking of chitosan by microwave assisted synthesis. *Sci. Int.* **2018**, *6*, 18–30. [CrossRef]
33. Ren, Q.; Zhu, X. Methyl-beta-cyclodextrin/cetyltrimethyl ammonium bromide synergistic sensitized fluorescence method for the determination of levofloxacin. *J. Fluoresc.* **2016**, *26*, 671–677. [CrossRef] [PubMed]
34. Cakmak, A.; Cirpanli, Y.; Bilensoy, E.; Yorganci, K.; Calis, S.; Saribas, Z.; Kaynaroglu, V. Antibacterial activity of triclosan chitosan coated graft on hernia graft infection model. *Int. J. Pharm.* **2009**, *381*, 214–219. [CrossRef] [PubMed]
35. Sanbhal, N.; Mao, Y.; Sun, G.; Xu, R.F.; Zhang, Q.; Wang, L. Surface modification of polypropylene mesh devices with cyclodextrin via cold plasma for hernia repair: Characterization and antibacterial properties. *Appl. Surf. Sci.* **2018**, *439*, 749–759. [CrossRef]
36. Blanchemain, N.; Haulon, S.; Martel, B.; Traisnel, M.; Morcellet, M.; Hildebrand, H.F. Vascular PET prostheses surface modification with cyclodextrin coating: Development of a new drug delivery system. *Eur. J. Vasc. Endovasc. Surg.* **2005**, *29*, 628–632. [CrossRef] [PubMed]
37. Laurent, T.; Kacem, I.; Blanchemain, N.; Cazaux, F.; Neut, C.; Hildebrand, H.F.; Martel, B. Cyclodextrin and maltodextrin finishing of a polypropylene abdominal wall implant for the prolonged delivery of ciprofloxacin. *Acta Biomater.* **2011**, *7*, 3141–3149. [CrossRef] [PubMed]
38. Debbabi, F.; Gargoubi, S.; Hadj Ayed, M.A.; Abdessalem, S.B. Development and characterization of antibacterial braided polyamide suture coated with chitosan-citric acid biopolymer. *J. Biomater. Appl.* **2017**, *32*, 384–398. [CrossRef] [PubMed]
39. Varshosaz, J.; Alinagari, R. Effect of citric acid as cross-linking agent on insulin loaded chitosan microspheres. *Iran. Polym. J.* **2005**, *14*, 647–656.

40. Sanbhal, N.; Saitaer, X.; Li, Y.; Mao, Y.; Zou, T.; Sun, G.; Wang, L. Controlled levofloxacin release and antibacterial properties of β-cyclodextrins-grafted polypropylene mesh devices for hernia repair. *Polymers* **2018**, *10*, 493. [CrossRef]
41. Sanbhal, N.; Mao, Y.; Sun, G.; Li, Y.; Peerzada, M.; Wang, L. Preparation and characterization of antibacterial polypropylene meshes with covalently incorporated β-cyclodextrins and captured antimicrobial agent for hernia repair. *Polymers* **2018**, *10*, 58. [CrossRef]
42. Nava-Ortiz, C.A.; Alvarez-Lorenzo, C.; Bucio, E.; Concheiro, A.; Burillo, G. Cyclodextrin-functionalized polyethylene and polypropylene as biocompatible materials for diclofenac delivery. *Int. J. Pharm.* **2009**, *382*, 183–191. [CrossRef] [PubMed]
43. Sarau, G.; Bochmann, A.; Lewandowska, R.; Christianse, S. From micro– to macro–Raman spectroscopy: Solar silicon for a case study. In *Advanced Aspects of Spectroscopy*; Farrukh, M.A., Ed.; IntechOpen: London, UK, 2012; pp. 221–246.